# A timetable rescheduling approach and transition phases for high-speed railway traffic during disruptions

**Journal Article**

**Author(s):**
Xu, Peijuan; Corman, Francesco (iD); Peng, Qiyuan; Luan, Xiaojie

# A Timetable Rescheduling Approach and Transition Phases for High-Speed Railway Traffic During Disruptions

Peijuan Xu, Francesco Corman, Qiyuan Peng, and Xiaojie Luan

**Research focused on the real-time rescheduling of high-speed railway traffic with a quasi-moving blocking system and transition process affected by the entrance delays and disruptions determining speed limitation. A mixed-integer linear program model related to a job shop model of operations is formulated to reduce the final delay (tardiness) of trains, where three objective functions combine different manners related to traffic control and speed management. The dynamic interaction between train speed and distance headway is considered in the model. Through experiments on a real-world high-speed line in China, the solution quality of the model is assessed by the delay distribution of trains or the smooth degree of train speed profile. The model manages to optimize traffic in the transition from a disordered condition (when disruptions appear) to a normal condition (after disruptions) for real-time operations. In conclusion, there are two and three transition phases for the cases without and with entrance delays, respectively, seen by analyzing the deviation between the rescheduled and planned timetables.**

Chinese high-speed railway faces a huge development for its efficiency, safety and punctuality. It is possible for passengers to reach their destination within a few hours by trains going at 300 km/h. However, sometimes trains are disrupted by unavoidable incidents or failures, disturbing railway operations and causing delays or even accidents. A high proportion of those disruptions results in train delays by reducing the maximum permitted speed of trains in a certain area. Because of the high frequency of these kinds of disruptions, a mathematical model is proposed that mitigates the negative influence on the traffic.

In the quasi-moving blocking system used in Chinese high-speed railway, the distance safety between two consecutive trains depends on the real-time speed of the trains. In regard to railway traffic rescheduling, the existing approaches apply either a fixed time interval or a constant space interval to separate trains, limiting their applicability to other situations, including the variable distance headway related to the quasi-moving block signaling. Furthermore, the methods related to the incorporation with speed optimization along traffic

management are also very rare. Moreover, few research works target the optimization within the transition phases during a disruption.

In light of that, proposed is a mixed integer linear programming (MILP) model to reduce the delay, considering speed management, when high-speed trains run under a quasi-moving block signaling system, and are affected by a speed limitation. The alternative graph model is extended to determine the number of the free sections in front of the train corresponding to its speed. The model was tested on a real-world network adapted from the Wuhan–Guangzhou high-speed railway in China with disruptions of different durations. The solution qualities of three objective functions are analyzed with regard to the tardiness and speed profiles, as well as the dynamics in the transition phases.

The key contributions of the research are as follows:

1. The transition phases for high-speed traffic during a disruption are considered and optimized, by evaluating the deviation in delay time along space or operation time.
2. The solution qualities of the model with two objective functions concerning traffic tardiness are comparatively evaluated in regard to final delays and delay distributions of trains.
3. An MILP model combining traffic control and speed optimization is developed based on the alternative graph method, a complement for the model in the paper (*1*).

The remainder of this paper is organized as follows. The next section presents a literature review studying the railway rescheduling problem, speed management, and transition processes during disruptions. Then, after a description of speed limitation, the MILP model is built, which reduces the delay of trains and manages train speed profiles. This is followed by the experiment and analysis of results. Finally, conclusions and directions for future research are reported.

## LITERATURE REVIEW

The adjustment of an online railway timetable to some unpredictable events such as disruptions or disturbances is currently a hot topic. Several approaches to optimization techniques are widely used to retime, reorder, or reroute the timetable and provide optimal strategies to restore the normal condition of the timetable, for example, microscopic and macroscopic methods. In regard to macroscopic methods, the event-activity method was applied to reschedule the timetables, to minimize train delays and the number of canceled trains in the case of a full blockage of open track (*2, 3*). The layouts of siding tracks and signals are neglected, as well as train speed. Zhan et al. (*2*) and Veelenturf et al. (*3*) considered the transition at the start of the

P. Xu and Q. Peng, School of Transportation and Logistics, Southwest Jiaotong University, No. 111, North First Section, Second Ring Road, Chengdu 610031, China. F. Corman and X. Luan, Maritime and Transport Technology Department, Delft University of Technology, Mekelweg 2, 2628 CD Delft, Netherlands. Corresponding author: Q. Peng, qiyuan-peng@home.swjtu.edu.cn.

disruption from the planned timetable to the disposition timetable, as well as the transition at the end of the disruption from the disposition timetable back to the planned timetable. More details on the transition phases are in the research (*3*).

Conversely, microscopic methods consider the detailed requirements of signals and switches, report precisely the headways between trains, and provide a more precise characterization of operations, at the cost of the increasing computation time. Railway operation was treated as a job shop scheduling problem, and the alternative graph was used for the conflict detection and resolution (*4–6*). The existing microscopic methods focus on dealing with minor perturbations, like entrance delay, blockage of one or several sections, instead of the full blockage of open track. A solution can be computed by exhaustive search approaches such as branch and bound, heuristics, metaheuristics, or commercial software like CPLEX. An alternative graph model targeted for the moving block signaling system, where a closed loop interaction optimized train speed according to a rescheduled timetable (*7*). As for optimization of train speed profiles, many research works aim to get an energy-efficient and continuous speed profile. For instance, Corman et al. studied the green wave in an alternative graph model (*8*), and Albrecht focused on optimizing the energy minimization problem to deliver a continuous speed profile, given a schedule (*9*).

For transition process under disruptions, the transition process for solving a railway disruption featured three phases from the normal timetable at the beginning of disruptions to the rescheduling timetable and then back to the normal condition after the disruption (*10*). Meanwhile, the bathtub model was used to illustrate the process, where the traffic experienced a decrease, a steady state valley with less traffic, and a final increase to normal operations (*11*). In this paper, it is assumed that the information on the disruption (duration, start time) is accurate, but added is further random dynamics through inclusion of entrance delay affecting the rescheduling process.

According to the foregoing analysis, iterative approaches are commonly used to combine the traffic management and speed control together, that is, a conflict-free timetable is computed in advance with a fixed-speed. In this paper, not only do the researchers integrate traffic management and speed control in one step, but they also try to optimize speed with a continuous and smooth profile. Finally, the transition process is also investigated to measure the robustness of the given timetable.

## PROBLEM DESCRIPTION AND MODEL FORMULATION

### Quasi-Moving Blocking System and Disruption Considered

The quasi-moving blocking system is widely used in the Chinese high-speed railway, which has similar function with European Train Control System (ETCS) Level 2, adjusting train speed according to distance headway between two trains to maintain train safety. Speed of trains is classified at five levels: 0–120 km/h, 120 km/h–200 km/h, 200 km/h–250 km/h, and 250 km/h–300 km/h, which need at least 1, 2, 3, 4, and 5 free sections in front of the train, respectively, for the requirement of braking distance, acceleration, and deceleration features of trains. With the implementation of this system, the variable distance headway has a profound impact on railway capacity, especially under the disruption determining speed restriction. According to the counted data related to disruptions (*12*), 85% of recorded disruption sources may result in speed limitation. As a

result, the focus is on reducing delay caused by disruptions related to speed limitations, by reordering trains and adjusting train speed to avoid conflicts beforehand. The disruptions considered are assumed to be given in the model, including the start time, duration, affected range, and maximum allowed speed level.

## MILP Model Based on Alternative Graph

### Conventional Alternative Graph Model

According to the microscopic approaches related to the job shop scheduling problem (*4*), railway networks can be described as an alternative graph ($G = \{N, F, A\}$) with arcs and nodes, where nodes denote sections separated by (virtual and real) signals and switches and arcs represent the direct connections between two successive sections. In a railway system, each section can only be occupied by one train at the same time, and the occupation for a section is called an operation. The minimum running time of one section for a train is called the operation time. The time when the train begins to use the section is named as the starting time. Let $N$ denote the set of nodes (sections); $F$ is the set of fixed arcs, representing the geographical connection between two sections (nodes) and guiding the route for each train; $A$ is the set of alternative arcs to avoid the potential conflicts between trains. The alternative arcs can determine the utilization order of one section for trains, to avoid the occupation of one section or the conflicting sections for two trains at the same time. Specifically, once one arc of each pair of alternative arcs is selected by one train, the other arc cannot be used at the same time. The alternative graph can be viewed as a disjunctive program and the typical formulations pertaining to operation time and alternative arcs are shown as Constraints 1 and 2.

$$\omega_{i,q} - \omega_{i,p} \geq f_p \qquad ((p,q) \in F) \tag{1}$$

$$(\omega_{j,q} - \omega_{i,p} \geq a_{pq}) \vee (\omega_{i,k} - \omega_{j,h} \geq a_{hk}) \qquad ((p,q),(h,k) \in A) \tag{2}$$

where

$\omega_{i,p}$ = starting time of train $i$ on section $p$, decision variables;
$f_p$ = operation time of section $p$;
$a_{pq}$ = time headway between two trains;
$i, j$ = index of trains; and
$p, q, h, k$ = index of sections.

Owing to the disjunctive relationship between two subconstraints in Constraint 2, the big $M$ is applied to reformulate them as constraints in Constraints 3 and 4.

$$\omega_{j,q} - \omega_{i,p} \geq a_{pq} - M(1 - \lambda_{i,j,p,q}) \qquad ((p,q),(h,k) \in A) \tag{3}$$

$$\omega_{i,k} - \omega_{j,h} \geq a_{hk} - M\lambda_{i,j,p,q} \qquad ((p,q),(h,k) \in A) \tag{4}$$

where $M$ is a sufficiently big value and $\lambda_{i,j,p,q}$ is a binary variable indicating the order of trains.

The selected arc from one pair of alternative arcs represents which train has the priority to use this pair of alternative arcs first. To be specific, if $\lambda_{i,j,p,q}$ is equal to 1 in Constraint 3, the time when train $j$ begins to use section $q$ should be at least $a_{pq}$ time units later than the time when train $i$ begins to occupy section $p$, that is, train $i$ precedes train $j$. Otherwise, Constraint 4 will be active and enforces the opposite order of trains.

Apart from this, the relevant constraints that restrict the entrance time (or entrance delay), dwell time, and departure time are consistent with the research work (*1, 4*).

### Improved Alternative Graph Model

In the formulation process involving traffic management and speed control, the following assumptions are made: the deceleration and acceleration profiles of trains are given, no trains are canceled during rescheduling process, the running time of each section for train depends on its real-time speed, and the granularity of time is 1 s.

The conventional alternative graph method is still available for the sections without speed concerned in the station area, but it is not capable to model the variable occupations of section in the open track area, taking the real-time (variable) speed of trains into account. As a result, an innovative alternative graph model was designed to address the variable distance headway depending on the train speed. First, the decision variables considered in this model are as follows:

1. $\omega_{t,s}$ denotes the starting time for train $t$ on section $s$, a real value.
2. $\lambda_{i,j,\vartheta}$, a binary variable with the similar function of $\lambda_{i,j,p,q}$ in Constraint 3, is used to indicate train order for the open track $\vartheta$, that is, if train $i$ is in front of train $j$, the value of $\lambda_{i,j,\vartheta}$ is equal to 1, otherwise $\lambda_{i,j,\vartheta} = 0$.
3. $\beta_{\xi,t,s}$, a binary variable, denotes the speed level $\xi$ of train $t$ on section $s$.
4. $\beta_{t,s}$ represents the finally selected speed level of train $t$ on section $s$.

The integration of speed control makes it possible to describe the influence of speed limitation with more variable parameters. As a result, the delay is caused by the extra running time owing to lower speed, as well as conflicts. Thus, the function of two objective functions is considered: reduction of final delay, the deviation between actual arrival time at the destination and planned arrival time. Objective 1 is to minimize the total delay time of all trains; Objective 2 minimizes the sum of the positive delay, shown as the objective functions 5 and 6, respectively. Objective 2 neglects the trains with early arrival, and it pays more attention to the delayed trains, balancing the early arrival and the delay.

$$\text{Objective 1: min: } \sum_{t\in T} \omega_{t,\text{end}} - e_{t,s} - c_t \tag{5}$$

$$\text{Objective 2: } \begin{cases} \text{min: } \sum_{t\in T} y_t \\ y_t \geq \omega_{t,\text{end}} - e_{t,s} - c_t & t \in T, s \in R_t \\ y_t \geq 0 & t \in T \end{cases} \tag{6}$$

where

$\omega_{t,\text{end}}$ = arrival time of train $t$;
$T$ = set of trains;
$R_t$ = route of train $t$;
$e_{t,s}$ = entrance time of train $t$ on the given entrance section $s$;
$c_t$ = planned total traveling time of train $t$; and
$y_t$ = positive delay times of train $t$, where negative delay is neglected.

Owing to the flexibility of the train profile, a train can accelerate to the maximum speed sharply, and after a short full-speed opera-

tion, it has to decelerate or stop quickly for some conflicts. This kind of speed profile results in high energy consumption and low comfort for passengers, so the further improvement in the speed optimization is considered in Objective 3. As given in current research, the generation of a continuous and smooth speed profile is a way to save energy. The aim of Objective 3 is to minimize the sum of the final delay and the transition times (acceleration and deceleration) of speed levels for all the trains, with the latter part smoothing the speed profiles, shown as the objective function 7. The coefficients $\gamma$ and $\chi$ are used to set the different weights for delay time and transition times of speed levels respectively. In the experiment, a detailed evaluation is given for $\gamma$ and $\chi$.

$$\text{Objective 3: min: } \gamma \cdot \sum_{t\in T} \omega_{t,\text{end}} - e_{t,s} - c_t + \chi \cdot \sum_{t\in T} \sum_{p,q\in G_\vartheta, (p,q)\in F} |\beta_{t,q} - \beta_{t,p}| \tag{7}$$

To clarify the working of this model, the relevant alternative graphs are plotted related to two trains (Train 1 and Train 2) on an open track, as illustrated in Figure 1. The geographic layout of track is reported by Figure 1*a*, where the range from Section 11 to Section 16 is a part of an open track with one-direction service. Figure 1*b* shows the layout of alternative arcs (red dash arcs connected by a circle) and fixed arcs (dark solid arcs) from the view of the traditional alternative graph model. Figure 1*c* shows a group of alternative arcs (colored arcs connected by a circle) of Section 11, which considers speed management and traffic control. Finally, the graph modeling speed optimization and traffic control is shown in Figure 1*d*. In Figure 1*b*, there is a pair of alternative arcs corresponding to each section to separate trains; the time headway between two trains is a fixed value $a_0$ and the minimum running time ($f_0$) for each section is uniform and fixed. Considering the overtaking on the open track is forbidden, the order of trains should be consistent for all the sections in one open track area. The final solution is composed of a series of selected arcs, coming from different alternative pairs, that is, only one arc is active in a pair of alternative arcs. This process can be achieved by Constraints 3 and 4.

In regard to Figure 1*c*, the red, purple, yellow, blue, and green dash lines denote 1, 2, 3, 4, and 5 available sections (the minimum distance safety) required by speed levels 1, 2, 3, 4, and 5, respectively; thus, there are 10 arcs (5 pairs) between two trains for entering one section. For simplicity, only the alternative arcs related to Section 11 are plotted. In the final solution, only one pair (represented by the same color) is active out of those 10 arcs, determining the speed; and a single arc in this active pair is selected to decide the train order. Meanwhile, the minimum running time of each section depending on the train speed level is determined, so the running time ($f_\xi$) above each fixed arc in the picture is variable. Note that $\xi$ denotes the selected speed level, $B = \{\xi | \xi = 1, 2, 3, \ldots, B_m\}$. The speed levels of two consecutive sections should be continuous, thus there is a feedback arc above two consecutive sections. The difference of speed level $\Delta \xi$ is applied to restrict this requirement, that is, $|\Delta \xi| \leq 1$. Additionally, the speed optimization is further achieved by restricting the summation of the changing times of speed levels ($\Sigma |\Delta \xi|$) for all the trains, as shown in Figure 1*d*. There is a new extra feedback arc at the top and bottom of Figure 1*d*, which is used to redistribute the speed levels of trains on each section, under the relevant restriction of railway capacity. In other words, the process to reduce the transition times of speed levels of a train is capable to smooth the train speed profile and improve the comfort level of passengers. Nevertheless, there is a complicated trade-off between the tardiness of traffic and the
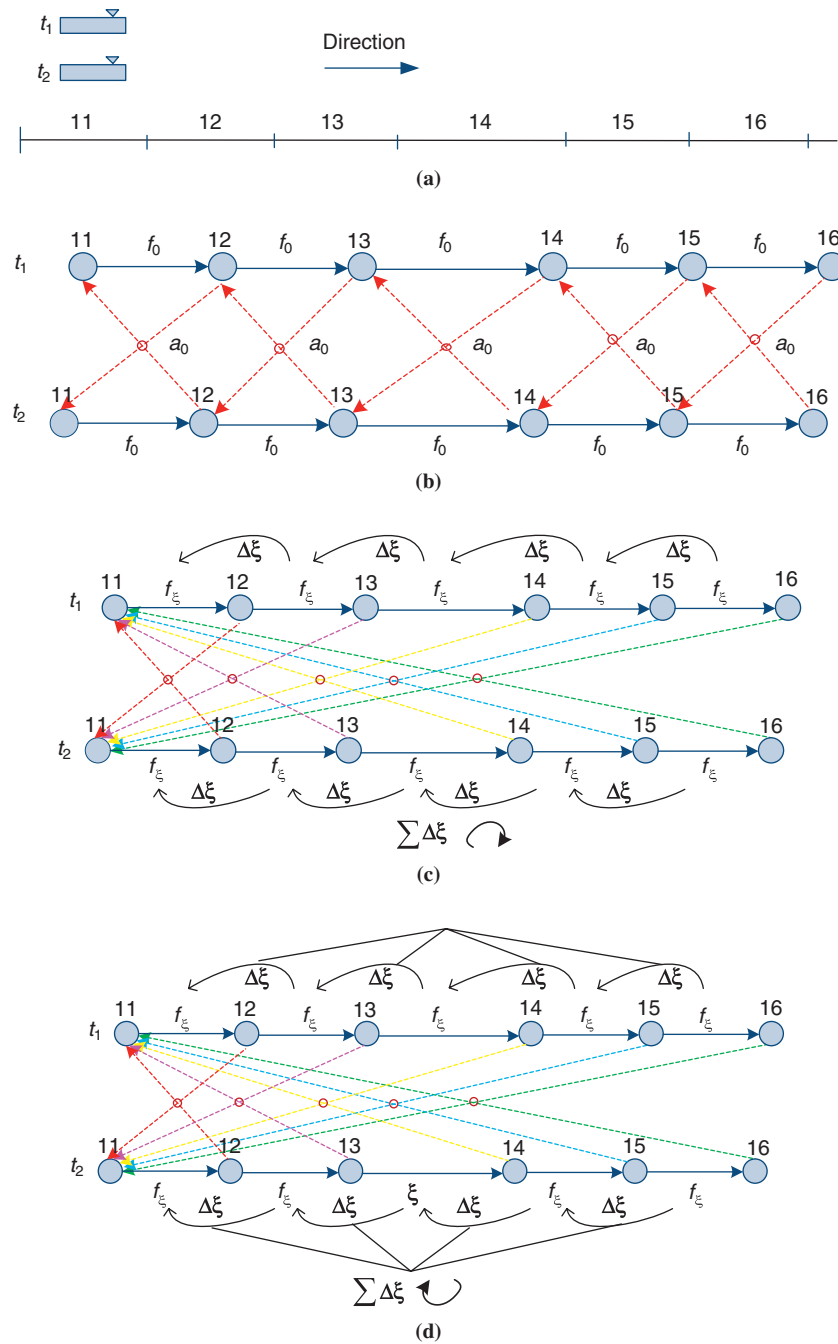
FIGURE 1   Layout of rail track and alternative graph: (a) layout of open track and two trains, (b) conventional alternative graph (without speed), (c) alternative graph considering speed management, and (d) alternative graph considering speed optimization.

smoothness of the speed profile. If traffic punctuality has priority, the optimal solution is one from the solution pool related to Figure 1c, with the minimum transition times of speed levels. The aim to adjust the coefficients of Objective 3 is to narrow the gap between the final delay of Objective 2 and Objective 3.

To fulfill the requirements of Figure 1, parts c and d, the researchers extend the original model by adding extra constraints. Specifically, Constraints 8 and 9 are used to adjust the minimum running times corresponding different speed levels, acting the same role as Constraint 1. Constraints 8 and 9 represent the least and largest threshold of running time corresponding to the speed level ξ. In this way $f_\varsigma$ is determined in Figure 1, parts c and d.

$$\omega_{t,q} - \omega_{t,p} \geq f_p + \sum_{\xi=1}^{B_m} \Delta t_\xi \beta_{\xi,t,p}$$

$$\forall t \in T,\, p,\, q \in \cup G_\vartheta,\, p,\, q \in R_t,\, (p,\, q) \in F \quad (8)$$

$$\omega_{t,q} - \omega_{t,p} < f_p + \sum_{\xi=2}^{B_m} \Delta t_{\xi-1} \beta_{\xi,t,p} + M\beta_{1,t,p}$$

$$\forall t \in T,\, p,\, q \in \cup G_\vartheta,\, p,\, q \in R_t,\, (p,\, q) \in F \quad (9)$$

$$\omega_{j,q} - \omega_{i,p} \geq -\left(2 - \lambda_{i,j,\vartheta} - \beta_{\xi,i,q}\right)M$$

$$\forall i,\, j \in T,\, \xi \in B,\, p,\, q \in G_\vartheta,\, q \in R_j,\, p \in R_i : i \neq j,\, p = q + \xi) \quad (10)$$

$$\omega_{i,q} - \omega_{j,p} \geq -\left(1 + \lambda_{i,j,\vartheta} - \beta_{\xi,i,q}\right)M$$

$$\forall i,\, j \in T,\, \xi \in B,\, p,\, q \in G_\vartheta,\, q \in R_j,\, p \in R_i : i \neq j,\, p = q + \xi) \quad (11)$$

where $G_\vartheta$ is the set of sections in the $\vartheta$th open track and $\Delta t_\xi$ is the additional running time related to speed level ξ.

In regard to the variable headway distance between two consecutive trains, Constraints 10 and 11 explain how the selection of alternative arcs related to speed work in one iteration. In this way, the headway time interval is replaced by the space interval. If $\lambda_{i,j,\vartheta}$ is equal to 1, there are at least ξ free sections between the former train i and successive train j with speed level at ξ; otherwise, Constraint 11 will be active, where the order between those two trains is reversed. Those two constraints make the selection of colored alternative arcs in Figure 1, parts c and d, possible.

$$\sum_{\xi=1}^{B_m} \beta_{\xi,t,s} = 1 \qquad \forall t \in T,\, s \in G_\vartheta,\, s \in R_t \quad (12)$$

$$\beta_{t,s} = \sum_{\xi=1}^{\xi=B_m} \xi \cdot \beta_{\xi,t,s} \qquad \forall t \in T,\, s \in G_\vartheta,\, s \in R_t \quad (13)$$

$$\beta_{t,q} - \beta_{t,p} \leq 1 \qquad \forall t \in T,\, p,\, q \in G_\vartheta,\, p,\, q \in R_t,\, (p,\, q) \in F \quad (14)$$

$$\beta_{t,q} - \beta_{t,p} \geq -1 \qquad \forall t \in T,\, p,\, q \in G_\vartheta,\, p,\, q \in R_t,\, (p,\, q) \in F \quad (15)$$

In addition, one section corresponds to only one speed level as shown in Equation 12, and the final selection for speed level $\beta_{t,s}$ is computed by Equation 13. Finally, the transition rule of speed levels on two consecutive sections is reported by constraints in Constraints 14 and 15.

## COMPUTATIONAL EXPERIMENTS ON REALISTIC HIGH-SPEED RAILWAY

To solve the MILP model, the commercial software IBM ILOG CPLEX 12.6 is considered with the default values. Experiments are all performed on a laptop with an Intel Core i7-5600U processor CPU 2.60GHz 8.00GB RAM. The experiments are done with a real homogeneous timetable, that is, a part of high-speed railway from Wuhan to Guangzhou. Since Chinese high-speed railway lines are all double-track lines and two tracks in different directions are independent, the researchers considered only the downward high-speed rail line. A two-step method is applied to accelerate the solving process (1), and the maximum computation time is set at 10 min.

### Test Instance and Parameter Values

Figure 2 shows part of the timetable from Hengyang (shown) to the north of Guangzhou (not shown), with six railway stations and six open tracks, which is part of the Wuhan–Guangzhou high-speed railway in China. There, 20 high-speed trains (300 km/h) are scheduled in the time span (9:00 to 11:00). The range of target track is exactly the scope of responsibility of one train dispatcher post. The number of siding tracks in each station and number of sections in each open track area are reported at the bottom of Figure 2. The total number of sections is 374. The length of each section refers to 1,360 m, and the minimum running time is 16 s for a train with a speed at 300 km/h. Additional running time intervals vary with different speed levels, that is, the speed levels ξ = 1, 2, 3, 4, 5 correspond to [24 s, +∞), [14 s, 24 s), [8 s, 14 s), [3 s, 8 s), [0, 3 s), respectively. The shaded rectangles in Figure 2 are the times and range extensions of speed limitations affected by disruptions, which occur at 9:00, and there are 50 sections disturbed in the open track (Leiyang–Chenzhou). The worst allowed speed (ξ = 1) and three durations (0.5 h, 1 h, and 1.5 h) are studied, respectively. In the experiments, trains in a time span of 2 h, whose starting time is consistent with the starting time of speed limitation, are considered. In the model, the number of variables in the experiment is 51,000, with 602,208 constraints. Furthermore, there are 20 cases with different entrance delays for each speed limitation, and the parameters (β = 1.48, η = 560, γ = 205) of entrance delay come from a Weibull distribution (13). The researchers report on the average over those 20 cases when not stated otherwise. The average value of 20 groups of entrance delays is 6,220.9 s. A case without any entrance delay, that is, punctual timetable, is tested as well.

### Analysis of Delay Difference with Different Objectives

In this section, the disruption with 0.5 h duration is tested. First, the difference between Objective 1 and Objective 2 is analyzed based on the final solution. In regard to the solution process, the average computation times of the two objectives are 172.52 s and 140.69 s, respectively. It is remarkable that it is easier for Objective 2 to get the optimal solution, compared with Objective 1. There are about 990 s and 722 s of delay times reduced by Objective 1 and Objective 2, respectively, compared with the solution based on the scheduling rule that maintains the same order as with the original timetable. This quantifies the benefits of the proposed model.
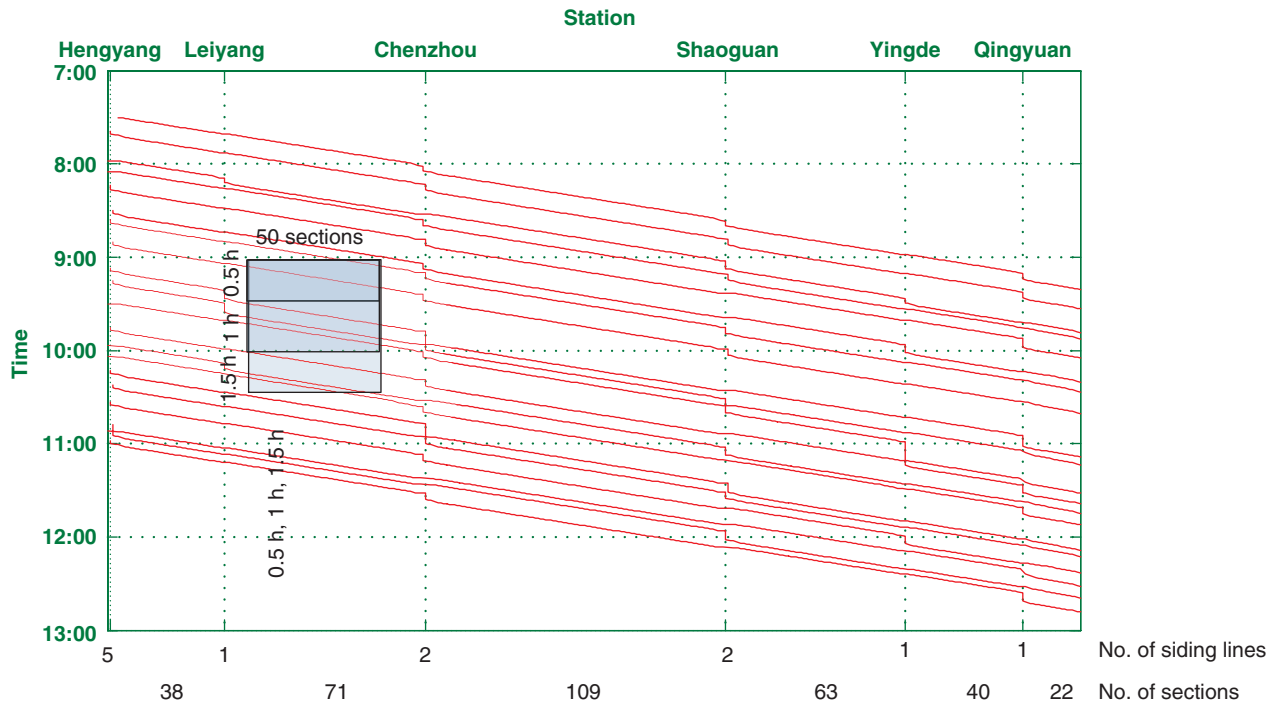
FIGURE 2   Planned timetable of target railway line.

The actual final delay of each train is analyzed, based on the optimal solutions of the two objectives. Figure 3 shows the delay time distribution of trains for the two objective functions. The box plots in Figure 3, *a* and *b*, report the median value, first and third quartiles, as well as the maximum and minimum values. In the first two subgraphs, the range of delay (the span between the minimum and maximum values) for each train in Figure 3*a* is similar to that of Objective 2 in Figure 3*b*. The median value of Objective 2 is a bit larger than that of Objective 1, while the extents of bars depending on the first and third quartiles are more compact than that in Figure 3*a*. It is can be concluded that the median of final delay shows a better quality in Objective 1 for the contribution of more negative final delays, while Objective 2 manages to provide a steadier solution with less fluctuation on the delays of trains. Apart from this, the top locations of bars related to Trains 7 and 8 reflect the influence of speed limitation, where about 500 s for each train are affected.

However, the probability distribution of final delays of each train is plotted in Figure 3*c,* where the *x*-axis represents final delay times in seconds, and the *y*-axis denotes probability. As seen in the figure, 80% of delays are less than 460 s. Concerning the trains with early arrivals—those with negative final delays—the results of those two objective functions are different, according to the probability distribution curves, that is, the probability of early arrival of trains from the solution of Objective 2 is less than that of Objective 1. Even though some negative final delays are neglected in the Objective 2 model, this does not mean that trains are not exploiting it; it is just not reported in the objective value. The probability of trains with positive delays is larger in Objective 2, with the major difference located in the range of 0–150 s. With values of delay time greater than 150 s, the curve related to Objective 2 shows only a slightly larger proportion than that of Objective 1. In this way, the difference in the components of solution between those two objectives is clarified. When one deals with speed limitation and large entrance delay,

Objective 1 is a better choice; Objective 2 is more suited to solve the slight disruption to avoid much earlier arrivals of trains.

## Optimization of Train Speed

Recall that Objective 3 integrates the traffic management and speed optimization into a single model by means of introducing coefficients $\gamma$ and $\chi$. Because of the trade-off relationship between transition times of speed levels and the traveling time, adjusting the coefficients is an efficient way to find a balance in those factors. With the aim to find the best continuous speed profiles under the minimum final delay, the combinations of $\gamma + \chi$, that is, $1 + 1$, $1 + 0.5$, $0.5 + 1$, are evaluated in Objective 3. The disruption concerned is consistent with that in an earlier section of the paper. Three groups of tests with regard to Objective 3 are performed. During the solving process, there is a large time consumption to improve the lower bound to reach the upper bound and their computation time (376.55 s) is longer than that of Objective 1 and Objective 2. According to the final solutions, the values are analyzed in regard to the total final delay and total transition times of speed levels independently. At the same time, the solution of Objective 1 is used to benchmark the solution of Objective 3, so the transition times of speed levels in Objective 1 are counted as well. The comparison results, that is, the average values of 20 cases with different entrance delays, are reported in Figure 4*a*.

As shown in Figure 4*a*, the blue line represents the final delays of the objective functions and the red line denotes the amount of transition times related to speed levels. The blue line shows final delay of the optimal solution is 2,384.27 seconds, computed by Objective 1, and the best solution among the three alternative objectives related to Objective 3 is 2,387.24 s, computed by Objective 3 with $1 + 0.5$ ($\gamma = 1$, $\chi = 0.5$). The final delay of the objective related to $0.5 + 1$
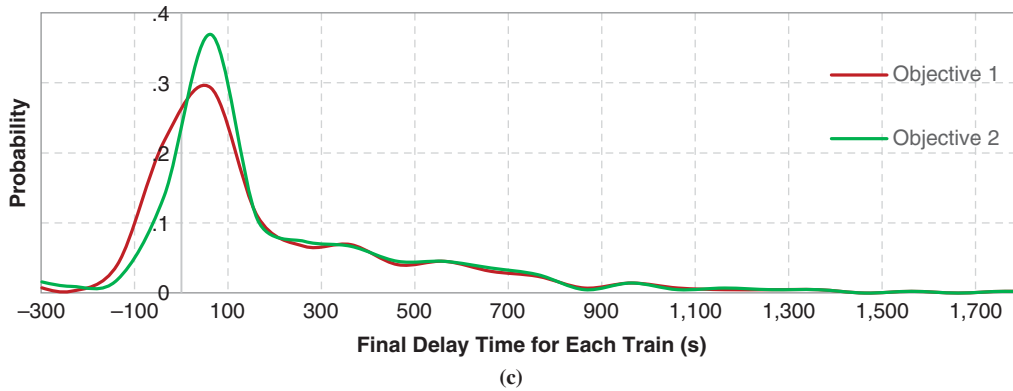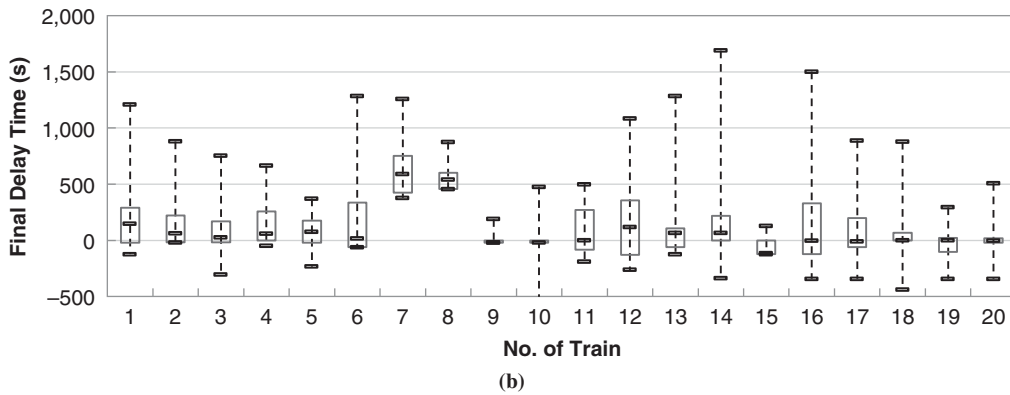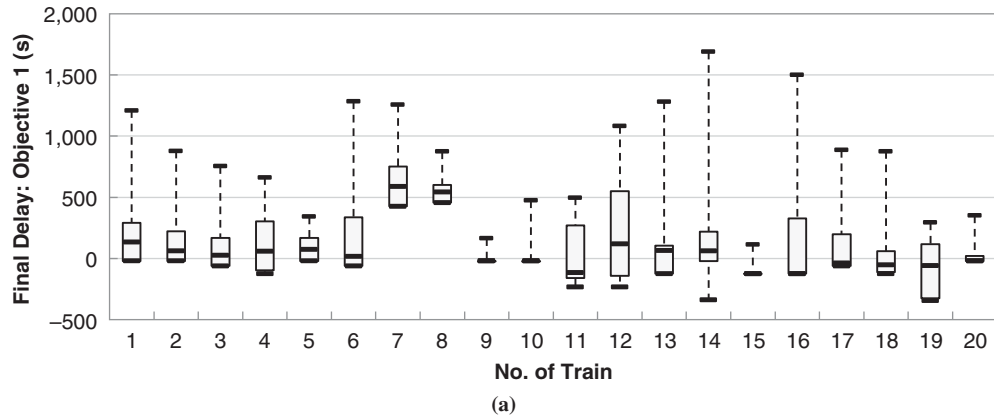
FIGURE 3  Analysis on final delay of each train: (*a*) range of final delay for each train in Objective 1, (*b*) range of final delay for each train in Objective 2, and (*c*) final delay distributions for Objective 1 and Objective 2.
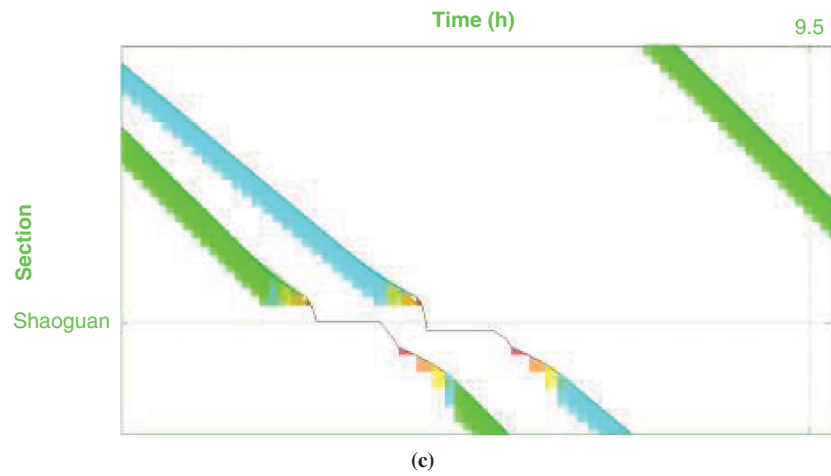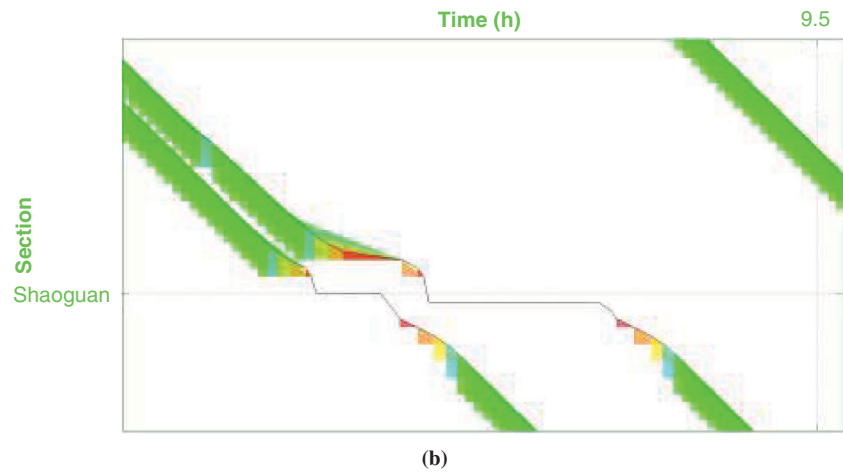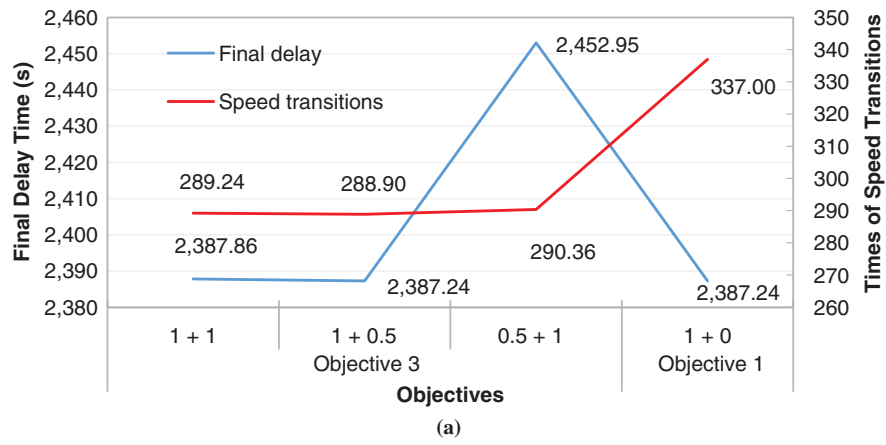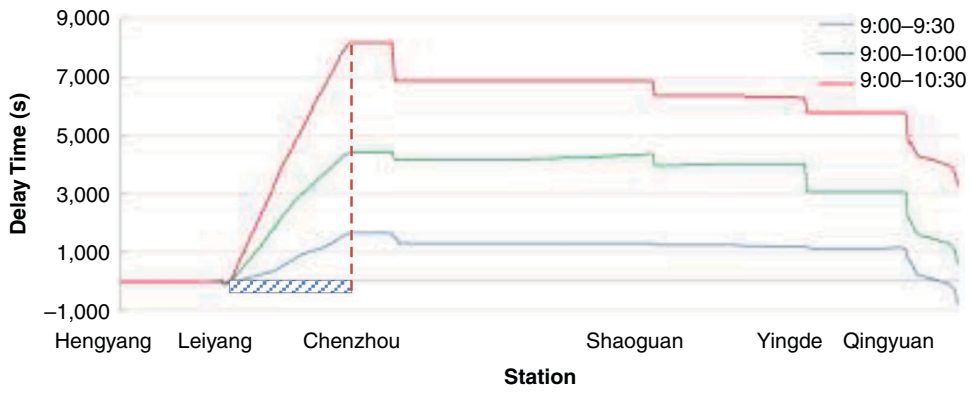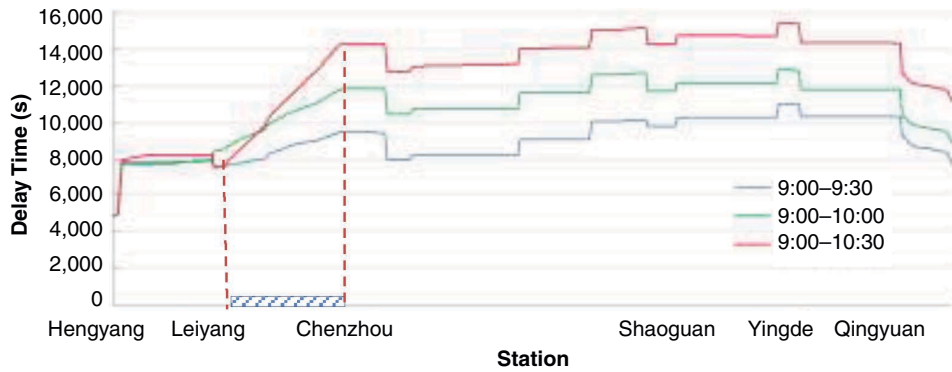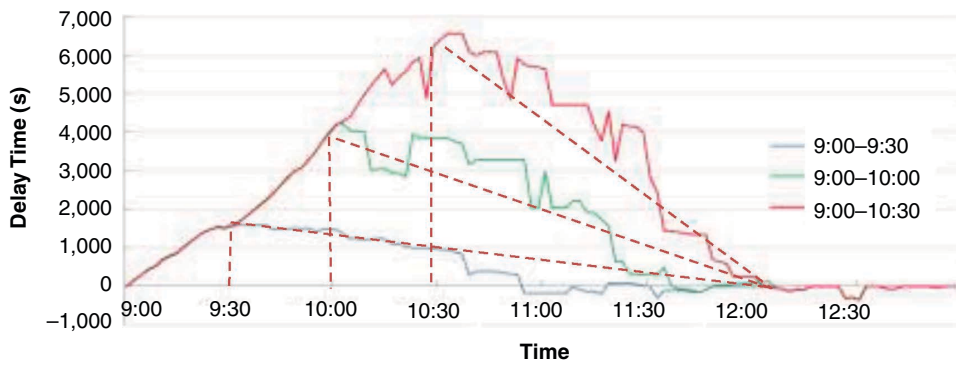
(a)



(b)



(c)

FIGURE 4   Comparison related to final solutions of Objective 1 and Objective 3:
(a) analysis for relevant results of Objective 1 and Objective 3, (b) timetable and speed
profiles based on Objective 1, and (c) timetable and speed profiles based on Objective 3.
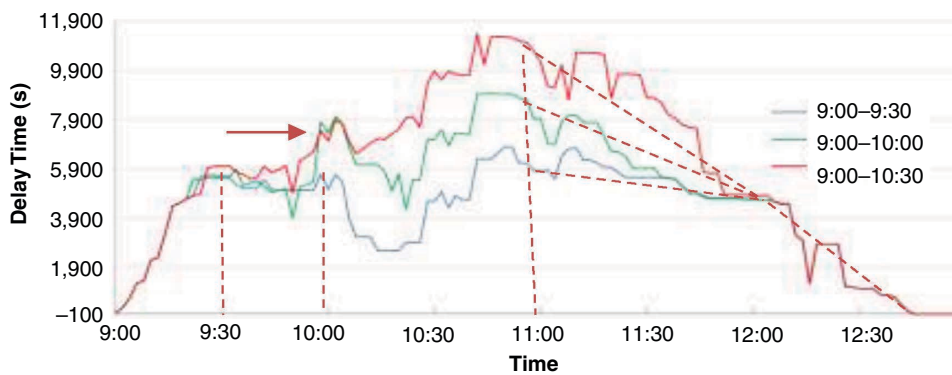
FIGURE 5   Deviation in delay along space and operation time: (*a*) deviation along space based on a punctual timetable, (*b*) deviation along space based on the timetable with entrance delay, (*c*) deviation along operation time based on a punctual timetable, and (*d*) deviation along operation time based on the timetable with entrance delay.

shows the worst with 2,452.95 seconds. Concerning the red line in regard to transition times, the least value (288.9) is computed by Objective 3 with 1 + 0.5 and the results of the other two combinations related to Objective 3 are higher; for Objective 1, the transition times of speed levels are about 377. One can conclude that the transition times of speed levels of Objective 1 are more frequency than trains actually needed during operation, and the three alternative models related to Objective 3 all can improve the performance of speed profile. Considering the final delay and speed performance together, Objective 3 with 1 + 0.5 is the best choice, regardless of the time consumption. Furthermore, the graphical illustration for the strength of Objective 3 in the rescheduled timetable is compared in Figure 4, parts b and c. For clarity, three running lines of trains, when they exit the impacted sections, are partially plotted. Figure 4b reports a result of Objective 1, and Figure 4c corresponds to the result of Objective 3 with 1 + 0.5. In Figure 4b, the second train has to stop (the second line with red color) and waits before it arrives at the next station, owing to the insufficient operation time of infrastructure. However, in Figure 4c, the second train runs at a lower speed (the second line with blue color) continuously to dwell at the next station without extra stop before it arrives. With the same traveling time, the later rescheduled timetable can save more energy and provide better service for passengers.

## Delay Analysis for Different Transition Phases

The target disruptions related to speed limitations have different durations: 0.5 h, 1 h, and 1.5 h. Two timetables, one with the punctual traffic and another with 10,031 s entrance delay, are considered. To better understand the transition process of the traffic during disruption, the researchers plotted the deviation of delay times along space and operation time between the rescheduled and planned timetables, as shown in Figure 5, where the red, green, and blue lines represent the deviation values related to 1.5-h, 1-h, and 0.5-h disruptions, respectively. Figure 5, parts a and b, reports the delay deviation (on the y-axis) along the track network (on the x-axis, where the intermediate stations are labeled, respectively, as well as the affected sections under the shadow). Figure 5, parts c and d, reports the delay deviation along the operation time (on the x-axis). Additionally, Figure 5, parts a and c, corresponds to the consequence of a punctual timetable, and Figure 5, parts b and d, relates to the timetable with entrance delay.

As shown in Figure 5, parts a and b, it is evident that the new initial delay (caused by speed limitation) is generated on the affected sections, as three lines rise dramatically with different slopes and reach their peaks at the last affected section. After trains exit the affected area, the delays propagate forward and decline slightly by using the recovery time in the timetable. In Figure 5a, the disrupted timetable recovers to the planned timetable behind Qingyuan station, when the disruption duration is 0.5 h. Instead, the cases with 1-h and 1.5-h disruptions need more space to restore a normal condition. Considering Figure 5b, the delay distribution resembles a wavy line behind Chenzhou station. After 9:00, trains enter the target railway network on different sections with different entrance delays; the deviation in final delay along railway line presents the comprehensive influence of speed limitation and entrance delays. Thus, with the discrete input of entrance delay, the transition process is disordered and extended to propagate geographically toward the farther track areas.

In regard to the delay propagation along time in Figure 5, parts c and d, each line has an approximate normal distribution pattern, no matter the case with or without entrance delay. In Figure 5c, the delay value rises with the time passing during the disruption. The three lines coincide until the end time of their corresponding disruptions and reach their respective peaks. Then three lines decline back to the normal condition by operational management. Those lines become more flexible in Figure 5d. Specifically, three lines with different duration times almost overlap together from 9:00 to 10:00. The gaps caused by different disruptions appear during 10:00 to 11:00 owing to the propagation of delay; then they reach the top value around 11:00. The punctual condition is restored only 1.5 h later. One can conclude that the entrance delay plays a huge role in the transition process by determining conflicts to prolong the influence and uncertainty of traffic.

On the basis of the foregoing analysis, the transition phases differ in the cases with and without entrance delays. There are two main phases for the rescheduling process without entrance delay, and instead three main phases for the process with entrance delay. In the case of the punctual timetable, the delay time is reduced efficiently after the disruption. The recovery time is determined by the severity of disruption. However, the entrance delay makes the solving process more complex, significantly disturbing the timetable. In the first phase, it is a gray area to estimate the disordered status and adjust traffic continuously. In the second phase, the delay increases because of the delay propagation, though the speed limitation is over. Graphically, the entrance delay causes the sway backward of the influence of speed limitation. Then it comes to the third phase, that is, the transition from the disrupted timetable back to a recovered original timetable.

In summary, analysis of the transition phases highlights the comprehensive and dynamic process of the combined influence of disruptions and entrance delay, and makes the impact of duration more specific. It is also feasible to measure the solution quality and robustness of the timetable. Moreover, in comparison with the transition process based on a punctual timetable, the timetable with entrance delay achieves a recovery to the normal condition in a longer and more uncertain way.

## CONCLUSION AND FUTURE RESEARCH

This paper focuses on the real-time rescheduling problem of a high-speed timetable and the transition process in regard to delay propagation in the geographic and time extension. To solve the problem caused by entrance delay and disruptions, an MILP model is proposed to reduce delay and applied to solve a real-world instance in an experiment, considering the quasi-moving block signaling system used in high-speed railways. Comparing three objectives in regard to final delays, the solution quality achieves some interesting implications about the delay distributions and the speed profile of each train. One can conclude that the transition process with entrance delay has three phases, which are more complex than the transition process under disruption but without entrance delays. Future research aims to exploit the transition process for the stochastic disruptions on the high-speed railway system, and to study more effective solution algorithms.

## ACKNOWLEDGMENTS

# REFERENCES

1. Xu, P., F. Corman, Q. Peng, and X. Luan. A Train Rescheduling Model Integrating Speed Management for Disruption Management of High-Speed Traffic Under a Quasi-Moving Block System. *Transportation Research Part B: Methodological,* 2016, under second review.
2. Zhan, S., L. G. Kroon, L. P. Veelenturf, and J. C. Wagenaar. Real-Time High-Speed Train Rescheduling in Case of a Complete Blockage. *Transportation Research Part B: Methodological,* Vol. 78, 2015, pp. 182–201. https://doi.org/10.1016/j.trb.2015.04.001.
3. Veelenturf, L. P., M. P. Kidd, V. Cacchiani, L. G. Kroon, and P. Toth. A Railway Timetable Rescheduling Approach for Handling Large-Scale Disruptions. *Transportation Science,* Vol. 50, No. 3, 2016, pp. 841–862. https://doi.org/10.1287/trsc.2015.0618.
4. D'Ariano, A., D. Pacciarelli, and M. Pranzo. A Branch and Bound Algorithm for Scheduling Trains in a Railway Network. *European Journal of Operational Research,* Vol. 183, No. 2, 2007, pp. 643–657. https://doi.org/10.1016/j.ejor.2006.10.034.
5. D'Ariano, A., F. Corman, D. Pacciarelli, and M. Pranzo. Reordering and Local Rerouting Strategies to Manage Train Traffic in Real Time. *Transportation Science,* Vol. 42, No. 4, 2008, pp. 405–419. https://doi.org/10.1287/trsc.1080.0247.
6. Corman, F., A. D'Ariano, D. Pacciarelli, and M. Pranzo. A Tabu Search Algorithm for Rerouting Trains During Rail Operations. *Transportation Research Part B: Methodological,* Vol. 44, No. 1, 2010, pp. 175–192. https://doi.org/10.1016/j.trb.2009.05.004.
7. Mazzarello, M., and E. Ottaviani. A Traffic Management System for Real-Time Traffic Optimisation in Railways. *Transportation Research Part B: Methodological,* Vol. 41, No. 2, 2007, pp. 246–274. https://doi.org/10.1016/j.trb.2006.02.005.
8. Corman, F., A. D'Ariano, D. Pacciarelli, and M. Pranzo. Evaluation of Green Wave Policy in Real-Time Railway Traffic Management. *Transportation Research Part C: Emerging Technologies,* Vol. 17, No. 6, 2009, pp. 607–616. https://doi.org/10.1016/j.trc.2009.04.001.
9. Albrecht, T. The Influence of Anticipating Train Driving on the Dispatching Process in Railway Conflict Situations. *Networks and Spatial Economics,* Vol. 9, No. 1, 2009, pp. 85–101. https://doi.org/10.1007/s11067-008-9089-0.
10. Louwerse, I., and D. Huisman. Adjusting a Railway Timetable in Case of Partial or Complete Blockades. *European Journal of Operational Research,* Vol. 235, No. 3, 2014, pp. 583–593. https://doi.org/10.1016/j.ejor.2013.12.020.
11. Ghaemi, N., and R. M. P. Goverde. Review of Railway Disruption Management Practice and Literature. *Proceedings of the 6th International Conference on Railway Operations Modelling and Analysis,* Narashimo, Japan, March 23–26, 2015.
12. Xu, P., F. Corman, and Q. Peng. Analyzing Railway Disruptions and Their Impact to Delayed Traffic in Chinese High-Speed Railway. *IFAC-PapersOnLine,* Vol. 49, No. 3, 2016, pp. 84–89. https://doi.org/10.1016/j.ifacol.2016.07.015.
13. Corman, F., A. D'Ariano, D. Pacciarelli, and M. Pranzo. Bi-Objective Conflict Detection and Resolution in Railway Traffic Management. *Transportation Research Part C: Emerging Technologies,* Vol. 20, No. 1, 2012, pp. 79–94. https://doi.org/10.1016/j.trc.2010.09.009.